



Received: 01.06.2024

Accepted: 23.06.2024

Research Article

In Silico Evaluation of Molecular Docking, Molecular Dynamic, and ADME Study of New Nabumetone Schiff Base Derivatives (1,3,4-oxadiazole or 1,3,4-thiadiazole ring) Promising Antiproliferation Action Against Lung Cancer

Ahmed Haloob Kadhim^{a, 1}, Monther Faisal Mahdi^a, Ayad Mohammed Rasheed^b

^aDepartment of Pharmaceutical Chemistry, College of Pharmacy, Mustansiriyah University, Baghdad, Iraq

^b College of Pharmacy, Al-Farahidi University, Baghdad, Iraq

Abstract: A total of eight novel Nabumetone Schiff Base Derivatives with 1,3,4-oxadiazole or 1,3,4-thiadiazole rings have been proposed to evaluate their potential effectiveness against the epidermal growth factor receptor (EGFR). Molecular docking was conducted with the crystalline structure of EGFR (code: 4HJO), wherein the eight compounds of Nabumetone Schiff Base Derivatives with 1,3,4-oxadiazole or 1,3,4-thiadiazole ring derivatives docked to determine their binding affinity to the target binding site. Using GOLD software (CCDC) version 5.43, computer predictions were made, and the compounds were designed using ChemDraw version 22.2 (professional version). Subsequently, their selectivity with EGFR was assessed, with erlotinib selected as a control for comparison. In silico ADME studies were conducted, revealing the significant potential for binding, and drug-likeness was assessed using the Swiss ADME website. Additionally, Molecular Dynamic simulations of compound N3 complexes with EGFR were performed using Schrodinger Suite 2023 software for 50 ns, estimating RMSD, RMSF, Ligand-Protein Contacts, and Ligand Torsion Profile results. Result Showing the best binding energy within receptor pocket with a promising activity against EGFR protein receptor. The highest PLP fitness levels were found in compounds N1, N2, and N3 for lung cancer cell protein (89.1, 89.02, and 87.95, respectively, average value), All compounds were found to adhere to Lipinski's rule of five, with high absorption from the gastrointestinal tract (except N4), and none of the proposed compounds were able to pass through the blood-brain barrier. Molecular dynamic result, Mean Protein RMSD 1.8 Å, ligand RMSD 1.6 Å, and RMSF reveals that the protein amino acids interacting with the ligand remain within a distance of less than 1 Å. In conclusion, these findings offer a promising direction for the development of effective treatments for lung cancer

Keywords: Nabumetone Schiff Base, 1,3,4-oxadiazole, 1,3,4-thiadiazole, Antiproliferation, EGFR protein receptor.

1. Introduction

Lung cancer is cancer that happens when abnormal cells grow in an uncontrol manner in the lung. It is a serious health problem that can lead to death. for a normal individual without these cells, the division is controlled. During the development of cancerous or malignant cells, the normal cell division is lost. Cells have changed in nature since transformations have happened in their genes (mutations have occurred). Also, the next generation of cancer cells is cancerous (1). The most prevalent forms of lung

cancer include non-small cell carcinoma (NSCLC) and small cell carcinoma (SCLC). Non-small cell carcinoma is more prevalent and tends to grow slowly, but small cell carcinoma is less common but overgrows (2). NSCLC, which accounts for approximately 85% to 90% of cases. Smoking is a major risk factor for NSCLC (3). The genes for the EGFR (epidermal growth factor receptor) family play an important role in NSCLC, their intervention is of significant interest in NSCLC treatment (4). The Food and Drug Administration has approved

¹ Corresponding Authors

e-mail: ahmed_haloub@uomustansiriyah.edu.iq

Ahmed Haloob Kadhim, Monther Faisal Mahdi, Ayad Mohammed Rasheed

erlotinib, a reversible tyrosine kinase inhibitor targeting EGFR used to treat NSCLC (5).

The tyrosine kinase receptor was found to be a central focus in cancer treatment. The protein receptor consists of an amino-terminal in the extracellular ligand-binding region, a hydrophobic trans membrane helix, and a domain within the cytoplasm (6). In regular cellular functions, EGFR facilitates the process which involves the transfer of phosphate from ATP to the tyrosine residue located within the catalytic kinase domain of EGFR. This action initiates a signaling cascade, which regulates essential cellular processes such as cellular cycle progression, motility of cells, invasion, and metastasis (7). Every alteration in the activity of EGFR kinase, whether because of over-expression or mutation, disrupts the normal signal transduction process, leading to the development of a cancerous state (8).

Efforts to block the EGFR pathway have been devised to impede tumor progression. One such strategy involves the utilization of small-molecule tyrosine kinase inhibitors to hinder EGFR expression. These inhibitors activate within the intracellular region of the receptor, competing against adenosine triphosphate by forming H-bonds and hydrophobic interactions within the ATP binding region of EGFR (9). This action displaces adenosine triphosphate, thereby inhibiting EGFR auto phosphorylation with subsequent downstream signaling pathways. The overexpression of EGFR in these tumors correlates with a poorer prognosis, making EGFR a prime target for anticancer therapy (10).

Researchers explored the correlation between H-bonding with the characteristics related to the anticancer activity. They discovered that the activity was enhanced when hydrogen-bonding donor groups were substituted at ring of the structure (11). The computational design of inhibitors can significantly expedite the process of developing drugs targeted at EGFR. It's widely acknowledged in clinical practice Protein kinase inhibitors play a significant impact in cancer treatment (12).

Studying the structure of the erlotinib and EGFR wildtype complex enables us to pinpoint the essential amino acid residues that engage with the inhibitor ligand. Molecular docking plays a crucial role as a valuable computational technique in drug

discovery, but it comes with a limitation: it offers only a static snapshot of the ligand-protein complexes. Multiple studies have proposed using molecular dynamics simulation (MD) to gain insights into the dynamic behavior of ligand protein complexes under a physiological environment (13). Molecular dynamics simulation can evaluate solvent effects in docked complexes, account for induced fit phenomena, compute free binding energies, accurately identify binding sites, and effectively dock ligands (14).

Moreover, a range of non-steroidal anti-inflammatory drugs, can notably impact the tumor microenvironment. They achieve this by decreasing cell migration, increasing apoptosis, and improving chemo-sensitivity (15).

Nabumetone Figure (1) a 1-naphthalenetic act as a NSAID that inhibits COX-2. Nabumetone shows anti-inflammatory pain relieving anticancer and chemo preventive exercises (16). In vivo Nabumetone inhibit intestinal carcinogenesis. In vitro this compound induces apoptosis in cancer cells of colon (16).

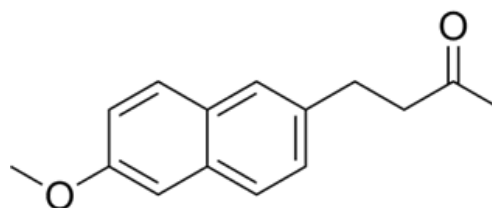


Figure 1. Nabumetone structure

Nitrogen-containing heterocyclic rings were being broadly investigated for their useful flexibility within the medication development particularly in anticancer research (17). N-heterocyclic skeletons encompass a diverse range of medical applications and serve as the foundational components for numerous contemporary drug candidates. This is attributed to the ability of nitrogen atoms within these structures to form hydrogen bonds with organic targets (18)

1,3,4-Thiadiazole ring Figure (2) which is part of the class of heterocyclic compounds, exhibit potential anticancer effects against certain cancer cell lines. These compounds interfere with the functioning of specific biological targets within cancer cells, thereby impeding the growth and progression of tumors (19)

Ahmed Haloob Kadhim, Monther Faisal Mahdi, Ayad Mohammed Rasheed

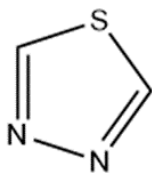


Figure 2. 1,3,4-thiadiazole ring

1,3,4-oxadiazole Figure (3) derivatives play a significant role in multi-directional biological activities. The anti-proliferative effects stem from various mechanisms, such as growth factor inhibition, enzyme regulation, and kinase activation. As a result, these compounds have been tested on various cancer cell lines (20).

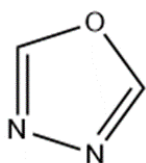


Figure 3. 1,3,4-oxadiazole

2. Computational Method

The design of the structure of proposed compounds (Nabumetone Schiff Base Derivatives) was informed by a thorough literature review conducted by our team, Figures (4 and 5). In silico modeling study was performed to find out the effect of proposed compounds on EGFR protein (Protein Data Bank ID: 4HJO). Using computational docking to uncover potential activity of our compounds compared with erlotinib, then studying how ligands interact with proteins. Molecular docking was done using EGFR protein as the first step to predict the fitness in protein cavity and the formation of Hydrogen bonds and other short contact within the protein cavity. Then study of

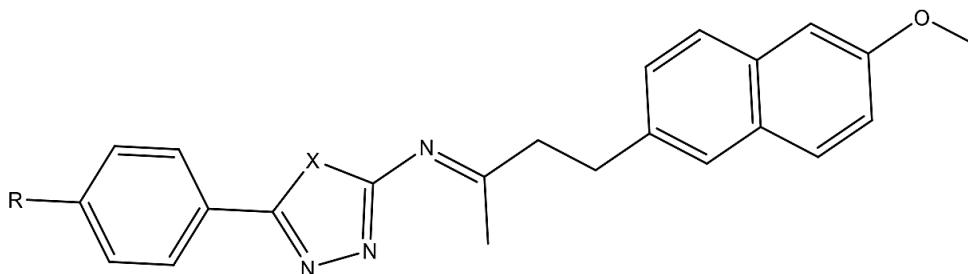
ADME properties of Compounds by using SwissADME server. Finally, molecular dynamics simulation was done by software Schrodinger Suite 2023 for uncovering the binding mechanism and conformational changes for the ligand protein complex in physiological environment by time (during 50 ns), Figure (4).

2.1. Preparation of Our Compound

Using ChemOffice software (ChemDraw 22.2.0) to draw the ligands' chemical structures (M1 to M8) and minimize the energy using Chem3D software to be ready for docking process.

2.2. Molecular Docking (Preparation of protein receptor for docking)

Three EGFR proteins were downloaded from the Protein Data Bank, namely 4HJO, to initiate the docking process. 4HJO, which represents the crystal structure of EGFR protein complexes with erlotinib. The target protein crystal structures were created by removing water molecules (Except essential water molecule HOH 1104 which is essential for activity for erlotinib by forming bridge with THR 830 and THR 766), Hydrogen atoms were included to ensure the appropriate ionization and tautomeric states of amino acid residues. The ligand docking process was conducted utilizing GOLD software (Hermes 2022.3.0) from the Cambridge Crystallographic Data Centre (CCDC). version with the full license used to prepare the receptor and make it ready for docking and for obtaining different poses for each compound. The GOLD docking procedure encompassed the binding site, incorporating all protein residues within a 10 Å radius of the reference ligands in the protein structure.



X= S , O

R= H, Cl, OCH₃, N(CH₃)₂, NO₂, CH₃

Figure (4): General structure of proposed Compounds

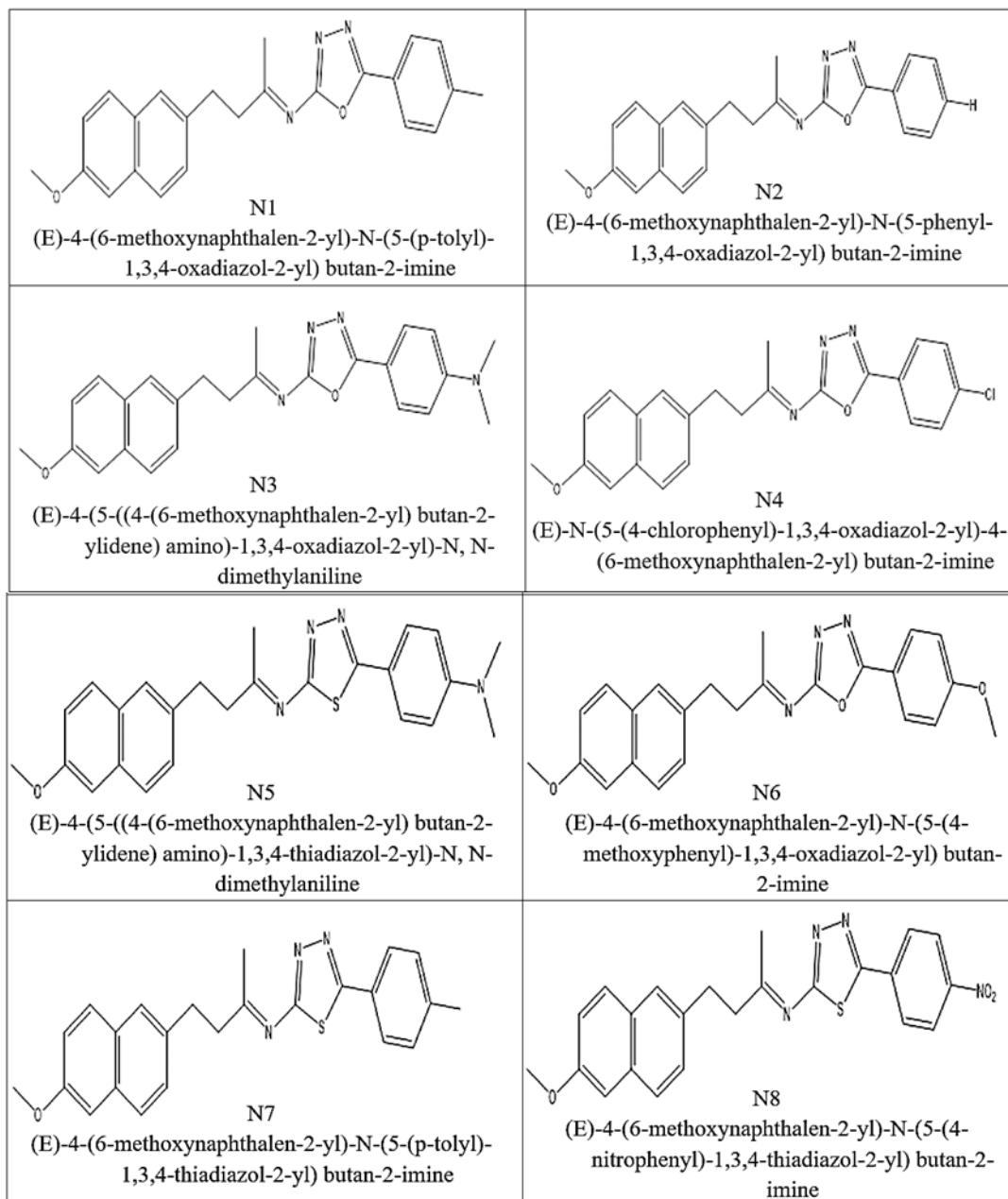


Figure (5): Structures of proposed Molecules

switching off the early termination, and resulted number done as ten. The default setting preserved the top-ranked solution, The ChemScore kinase configuration guide was used, and the ChemPLP fitness was used as the score function.

Running the software on Windows 10 operating system on the ASUS Laptop ROG Strix G G731 Intel Core i7- 9750 H CPU 2.60 GHz, 500GB SSD M.2, RAM 16 GB, NVIDIA GeForce RTX 2060).

2.3. ADME properties determination

This was done by using the SwissADME server, perform to estimate the pharmacokinetic profile of drugs that involve ADME (absorption, distribution, metabolism, and excretion), Additionally, other specifications, such as BBB (blood -brain barrier) penetration, P-gp affinity, and bioavailability, were evaluated. Which is Identifying the safety and eliminating compounds with poor ADME features, which were more likely to fail in later stages of the drug development process.

To design all compounds by using ChemDraw and by using the SwissADME server convert Compound to SMILE names.

2.4. Molecular Dynamics Simulation

MD simulations have become a well-established technique that can be effectively utilized to understand the interactions between macromolecular ligands and receptors. The outcomes of these simulations are comparable to biologically relevant findings. Additionally, unlike the relatively static molecular docking approach, MD modeling acknowledges the dynamic nature of proteins, considering that they change over time. Preparation of EGFR Protein done by Schrodinger Suite 2023 software, choose one complex for MD simulation using Desmond module, due to Docking result. Choice N3 compound for Molecular Dynamic process depend on Molecular Docking results, then designing the system using SPC water model in box with dimension 10 Å with OPLS4 force field. Neutralize with 0.15 NaCl at neutral PH, MD simulations were examined for a duration for 50 nanoseconds under a consistent temperature of 300 Kelvin.

3. Results and discussion

The aim is to create efficient and High-Precision Compounds with high selectivity characteristics and with good ADME properties.

3.1. Molecular Docking

Docking Results Virtual screening (VS) by using a computer software to find compound based on their fitting to the target receptor. Docking result determines hydrogen bound and short contact distance between protein atoms and ligands. The high number of Hydrogen bond interactions and hydrophobic interaction increase the biological activity which are needed for substrate for binding to active site (21,22).

The data acquired through molecular docking disclosed the binding energies associated with ligands binding to receptors. The resulted binding affinity (PLPfitness) average score for all compound table (1) and figure (6) found between 89 and 81 on EGFR while the erlotinib average score 74.75. The high score (PLPfitness) of proposed compounds (N1 to N8) because of an excellent binding affinity and good orientation within the binding site of receptor, the highest score 89.1, 89.02 and 87.95 for compound N1, N2 and N3 respectively between compounds as shown in the Table (1). The results from molecular docking indicated that these compounds had a strong binding affinity to EGFR, surpassing that of erlotinib, a standard control drug. This suggests the potential effectiveness of these compounds in interacting with EGFR, a critical target in lung cancer treatment.

Table (1); Molecular docking results against EGFR (PDB: 4HJO) using GOLD software

| No. | Ligand Name | PLPfitness (Average Values) | H-bond interactions | Hydrophobic interactions |
|-----|-------------|-----------------------------|--|--|
| 1 | Erlotinib | 74.75 | HOH 1104 bridge with THR 830 and THR 766 | GLY695 (2), CYS 773, ALA 719, LEU 834, HOH 1104 bridge with THR 830 and THR 766 |
| 2 | N1 | 89.10 | ASP 831, THR 830 | VAL 702, LYS 721 (3), ASP 831 (3), THR 830, MET 742 (2), PHE 832 (2), HOH 1104 bridge with THR 830 and THR 766 |
| 3 | N2 | 89.02 | ASP 831, THR 830 | ASP 831, THR 830, LYS 721, MET 742 |
| 4 | N3 | 87.95 | THR 830, LYS 721 (2), HOH 1104 bridge with THR 830 and THR 766 | VAL 702, LEU 721, MET 742 (3), LEU 753 (2), LEU 768 (2), THR 830 (2), LEU 820, LEU 834, HOH 1104 bridge with THR 830 and THR 766 |
| 5 | N4 | 86.90 | THR 830, HOH 1104 bridge with THR 830 and THR 766 | MET 742, THR 830, LEU 820, LYS 721, HOH 1104 bridge with THR 830 and THR 766 |
| 6 | N5 | 84.15 | HOH 1104 bridge with THR 830 and THR 766 | LYS 704, MET 742, LEU 764 (3), LEU 834 (5), THR 830, HOH 1104 bridge with THR 830 and THR 766 |
| 7 | N6 | 83.79 | LYS 721, HOH 1104 bridge with THR 830 and THR 766 | LEU 764, MET 742 (3), THR 830, HOH 1104 bridge with THR 830 and THR 766 |

Ahmed Haloob Kadhim, Monther Faisal Mahdi, Ayad Mohammed Rasheed

| | | | | |
|---|----|-------|--|---|
| 8 | N7 | 82.67 | LYS 704, THR 830, HOH 1104 bridge with THR 830 and THR 766 | VAL 702, LYS 704, THR 830, LEU 753, LEU 764 (4), ASP 831, LEU 820, HOH 1104 bridge with THR 830 and THR 766 |
| 9 | N8 | 81.49 | LYS 704 | LEU 768 (5), LEU 694, LEU 820, ASP 831, MET 742 (2), LEU 764 |

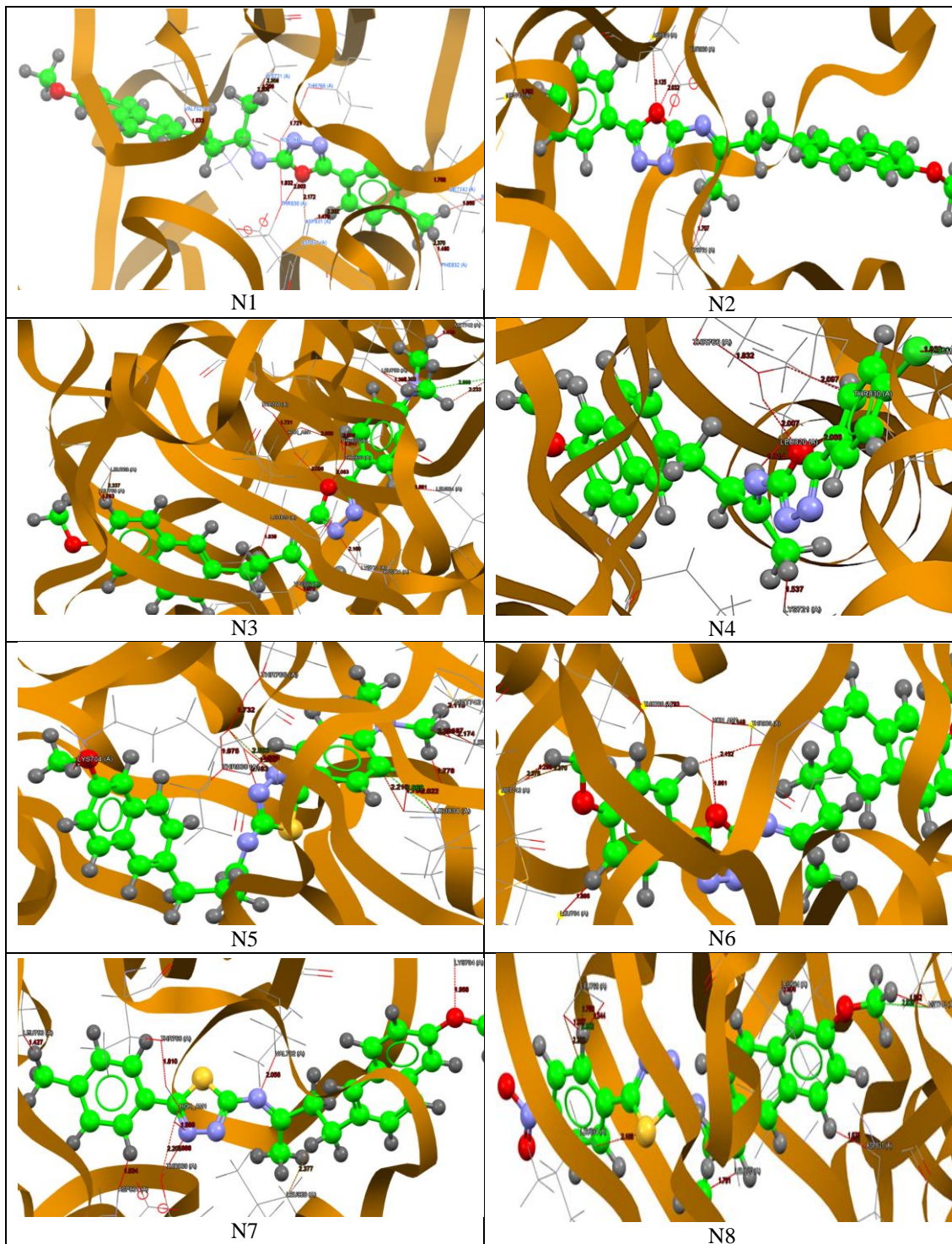


Figure (6); 3D intermolecular interactions of the best-docked complexes between proposed compounds and EGFR (PDB: 4HJO) using gold software

Ahmed Haloob Kadhim, Monther Faisal Mahdi, Ayad Mohammed Rasheed

Table 2. Lipinski's rule of for all compounds and control compound

| Compound | M.W | HBA | HBDs | LogP | Rotatable bonds |
|-----------|--------|-----|------|------|-----------------|
| Erlotinib | 393.44 | 6 | 1 | 3.67 | 10 |
| N1 | 385.43 | 5 | 0 | 4.53 | 6 |
| N2 | 414.50 | 5 | 0 | 4.19 | 7 |
| N3 | 405.88 | 5 | 0 | 4.56 | 7 |
| N4 | 432.49 | 6 | 0 | 4.46 | 7 |
| N5 | 401.52 | 4 | 0 | 3.65 | 6 |
| N6 | 401.52 | 4 | 0 | 4.44 | 6 |
| N7 | 430.57 | 4 | 0 | 4.48 | 7 |
| N8 | 430.57 | 4 | 0 | 4.66 | 7 |

MWT: molecular weight, HBAs: hydrogen bond acceptors, HBDs: Hydrogen bond donors, LogP: partition coefficient.

Table 3. Pharmacokinetics properties for all proposed compounds and control compound

| Name | MR | TPS(Å) | GI absorption | BBB permeability | BS | P-gp substrate |
|-----------|--------|--------|---------------|------------------|------|----------------|
| erlotinib | 111.40 | 74.73 | High | Yes | 0.55 | No |
| N1 | 116.81 | 60.51 | High | No | 0.55 | Yes |
| N2 | 111.85 | 60.51 | High | No | 0.55 | Yes |
| N3 | 126.06 | 63.75 | High | No | 0.55 | Yes |
| N4 | 116.86 | 60.51 | Low | No | 0.55 | Yes |
| N5 | 126.28 | 121.43 | High | No | 0.55 | No |
| N6 | 118.34 | 69.74 | High | No | 0.55 | Yes |
| N7 | 122.43 | 75.61 | High | No | 0.55 | Yes |
| N8 | 126.28 | 121.43 | High | No | 0.55 | Yes |

3.2. ADME

Important point needed for assessing the ADME properties in initial stages of research, ADME analysis sheds light on the compounds' pharmacokinetic properties, revealing favorable characteristics like good absorption and adherence to established drug design rules. Was done by using SwissADME server to estimate the properties of designed chemical compounds,

Lipinski's rule of five is increasingly favored in pharmaceutical research due to its effectiveness and cost-efficiency. Table (2) presents the results obtained from applying Lipinski's rule of five. These forecasts illustrate strict adherence to rule of five (Lipinski rule), with no observed violations in terms of MWT (molecular weight), HBDs (hydrogen bond donors), HBAs (hydrogen bond acceptors), and O/W (octanol/water) partition coefficient, and Rotatable bonds. (23).

Also predict the properties related to Bioavailability, TPSA (Total Polar Surface Area), Molar Refractivity, and pharmacokinetic properties. Predictions suggested minimal

penetration of the blood-brain barrier, which is advantageous in avoiding potential central nervous system side effects. Table (3).

3.3. Molecular Dynamic

Molecular dynamics (MD) simulation for a protein-ligand complex (N3-EGFR complex) revealed significant insights into dynamic behavior and the complex stability during time. The selection of N3 compound for Molecular Dynamics based on Molecular Docking results which show the same Hydrogen Bond result (HOH 1104 bridge with THR 830 and THR 766) for Erlotinib and having acceptable ADME results.

3.3.1. The RMSD:

The first result shows Root Mean Square Deviation (RMSD) over time, by measuring the average of changing at Angstrom during 50 nanoseconds in relocation of a selected atoms for a specific frame about a reference frame. RMSD values range between 1 to 3 Å, suggesting a well-balanced protein structure. Figure (7).

3.3.2. Protein RMSD

Tracking the Protein Root Mean Square Deviation offers a meaningful understanding of structural dynamics over the simulation process. Fluctuations range between 1-3 Å typically deemed acceptable for compact globular proteins. However, if the deviations exceed this range, it suggests significant

conformational changes taking place throughout the simulation. The graph illustrates the peaks in regions of the protein that undergo the most pronounced fluctuations. With an average Protein RMSD of 1.8 Å, falling within the normal range, it indicates the stability of the protein throughout the 50 ns duration. (Figure 7)

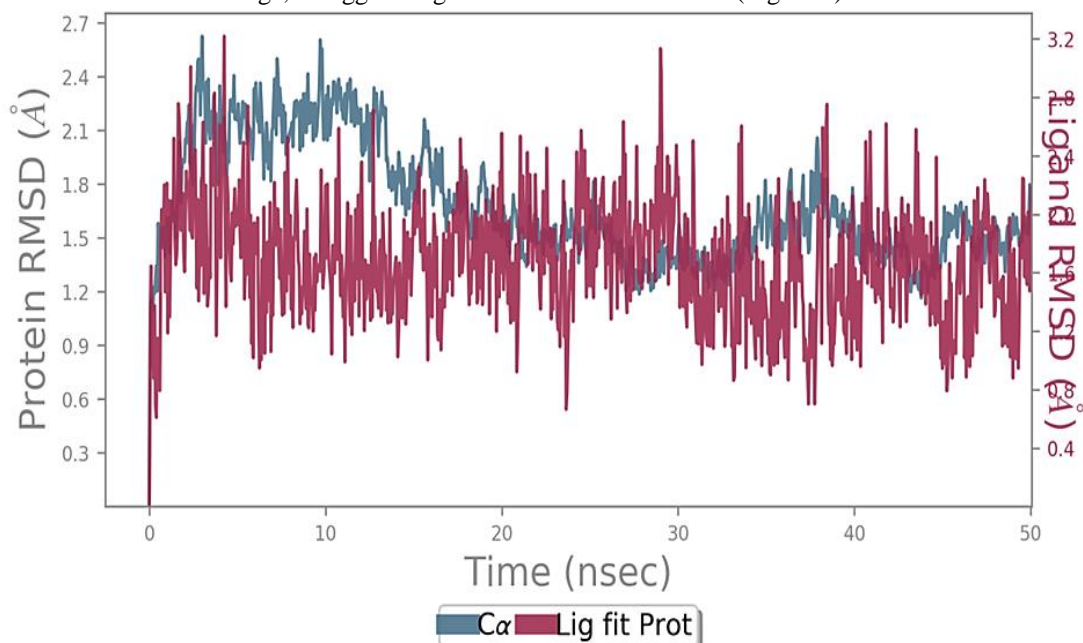


Figure (7); RMSD of the atoms of protein and the ligand over time (N3-EGFR).

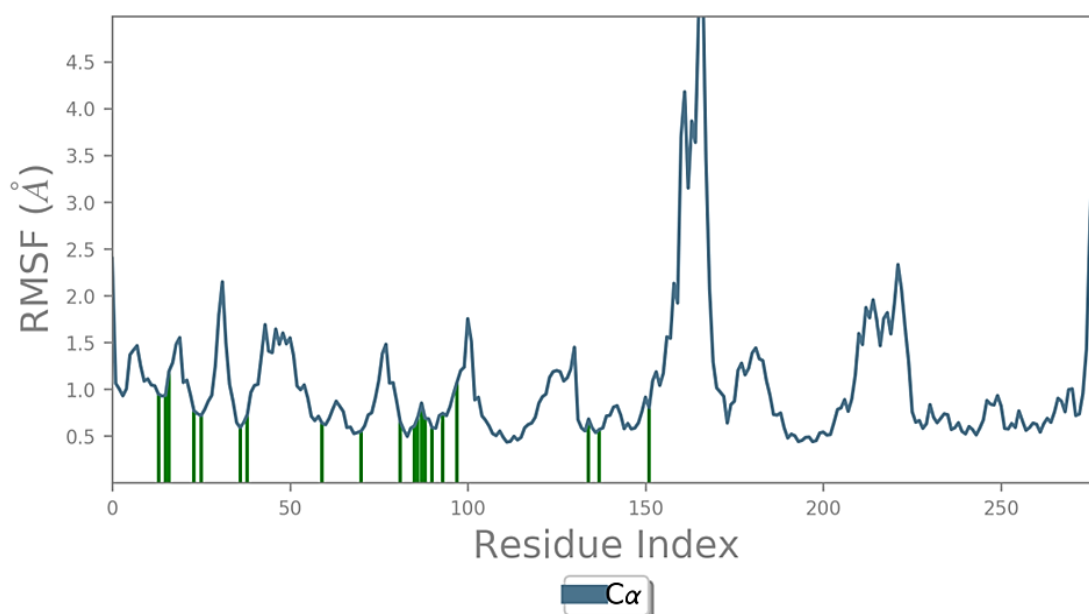


Figure (8); RMSF of protein (N3-EGFR).

3.3.3. Ligand RMSD

The Ligand RMSD evaluates the ligand's stability within the protein's binding pocket and its interactions throughout the simulation. This process

entails aligning the protein-ligand complex with the protein's reference backbone and computing the RMSD of the ligand's heavy atoms. Elevated values compared to the protein's RMSD may indicate

potential displacement of the ligand from its original binding site. Ideally, the ligand's RMSD should not exceed 2 Å. Indicating a stable complex with the protein. The results indicate a mean ligand RMSD line of approximately 1.6 Å. Which considered within the stable protein-ligand complexes range. (Figure 7)

3.3.4. Protein RMSF

The RMSF of the protein offers insights into localized changes along its chain during the

simulation. Peaks in the graph indicate areas where the protein experiences significant fluctuations. In the Ligand Contacts analysis, protein residues that interact with the ligand are represented by green vertical bars. The analysis reveals that the protein amino acids interacting with the ligand remain within a distance of less than 1 Å. Indicates the binding groups of N3 stable interact with protein amino acid. (Figure 8)

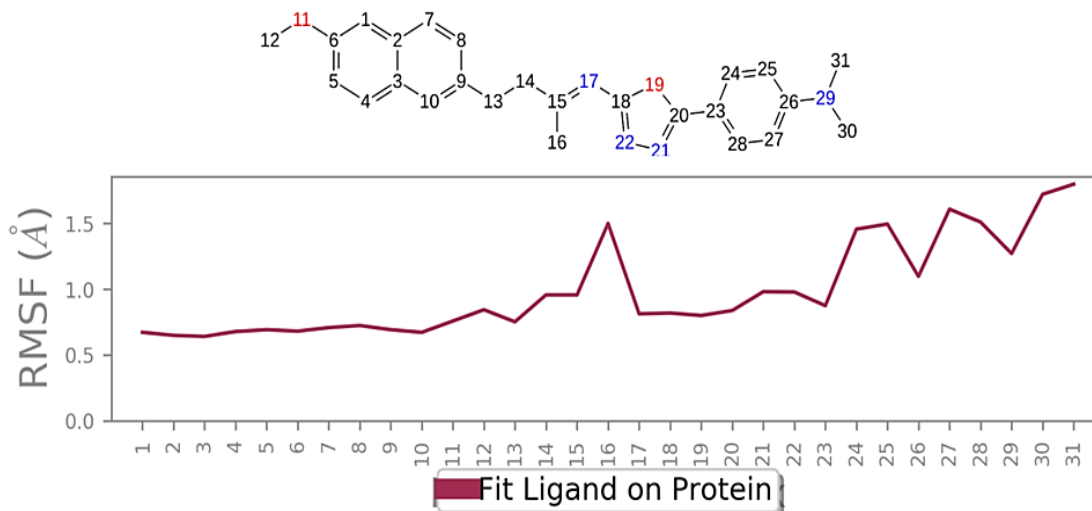


Figure 9. Ligand RMSF (N3-EGFR).

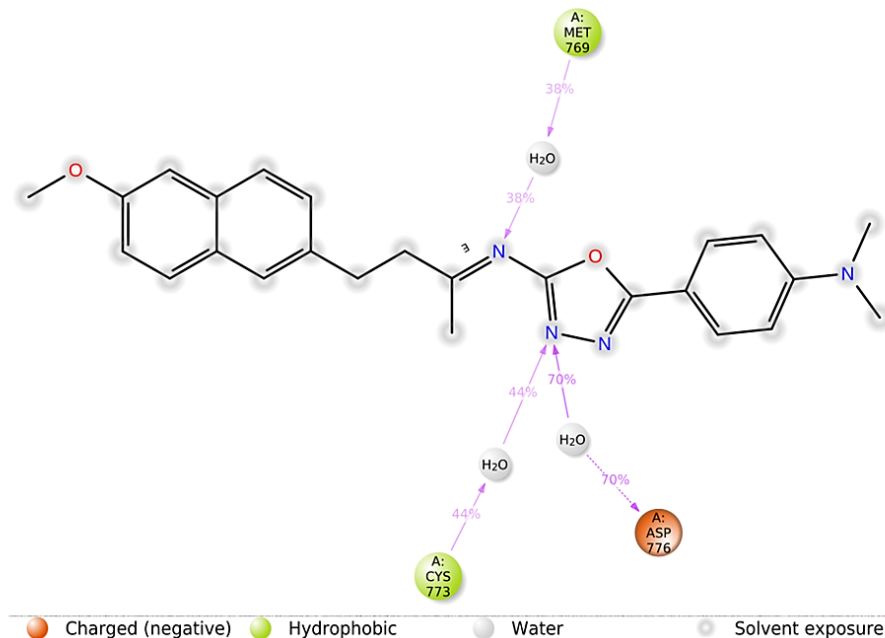


Figure (10); Ligand- Protein Contacts (N3-EGFR).

3.3.5. Ligand RMSF

The Ligand Root Mean Square Fluctuation (L-RMSF) is a beneficial metric to characterize alterations in the positions of ligand atoms

throughout the simulation. The ligand RMSF offers valuable insights into the interactions between ligand fragments and the protein, as well as their entropic impact on the binding process. Initially,

Ahmed Haloob Kadhim, Monther Faisal Mahdi, Ayad Mohammed Rasheed

the alignment of the protein-ligand complex relies on the protein backbone, followed by the assessment of the ligand's RMSF using its heavy

atoms. From the Figure (9) the Compound N3 RMSF results showed below 1.5 Å.

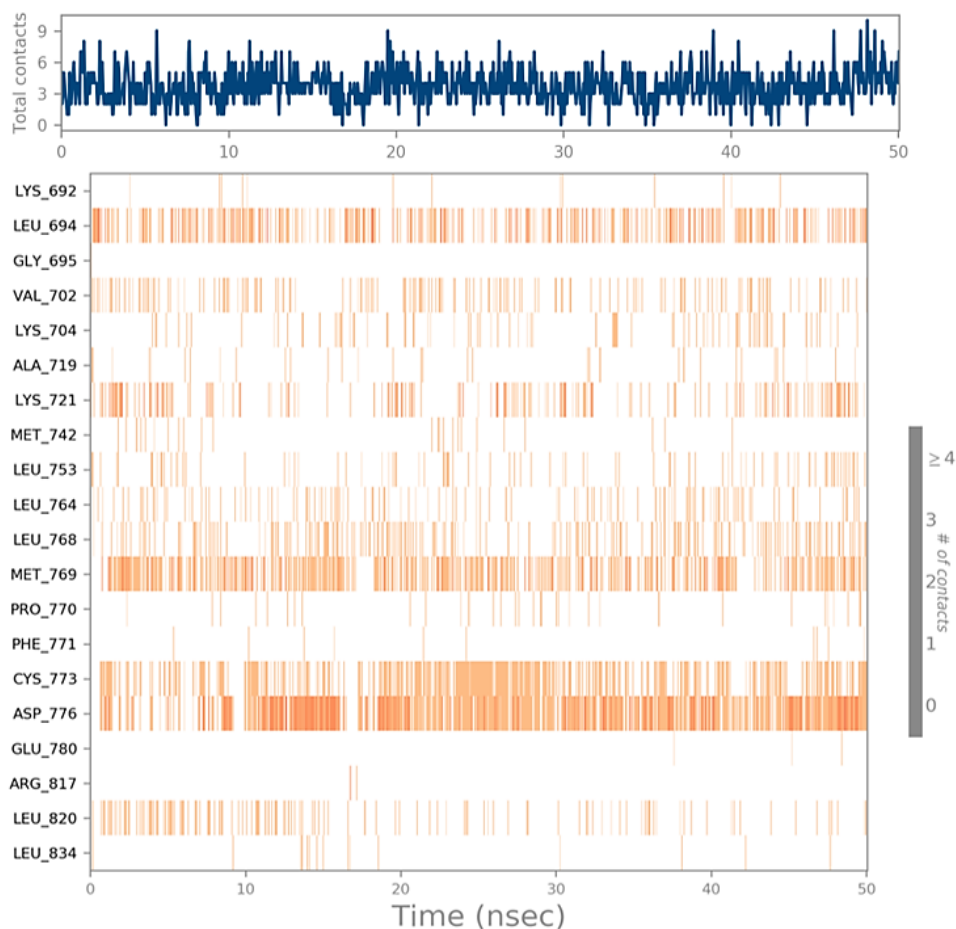


Figure (11); Protein-ligand interactions during Time (N3-EGFR).

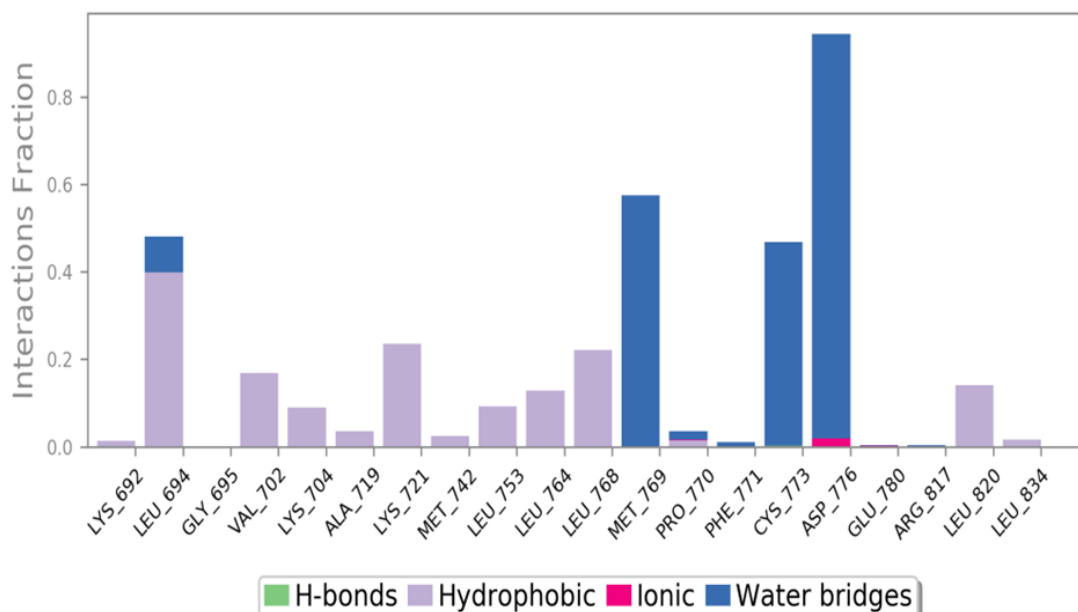


Figure (12); Protein-ligand contact histogram (N3-EGFR).

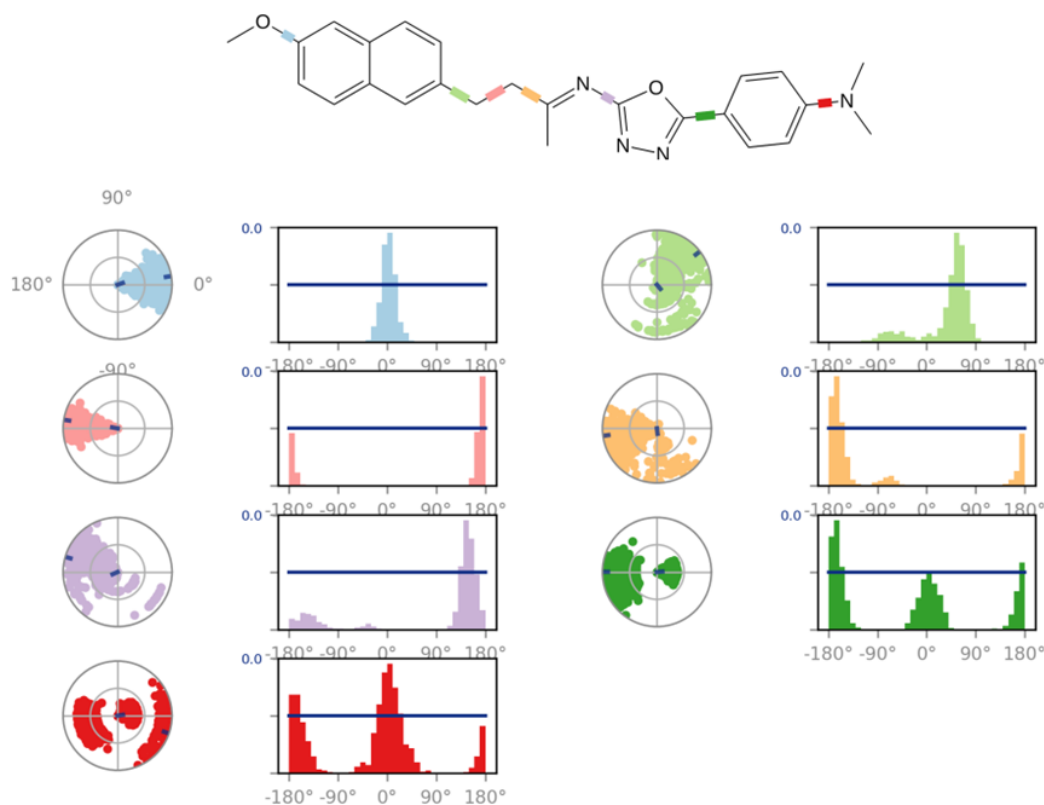


Figure (13); ligand Torsion Profile.

3.3.6. Ligand-Protein Contacts

A diagram illustrating the intricate interactions between ligand atoms and protein residues is presented. These interactions are defined by their occurrence for more than 30.0% of the simulation time within the chosen trajectory (0.00 through 50.05 nanoseconds). Figure 10 depicts the interactions with amino acid residues (MET 769 - 38%, CYS 773 - 44%, and ASP 776 - 70%), all facilitated through water bridging.

3.3.7. Protein-Ligand Contacts (cont.)

The figure presents stacked bar charts that depict the normalized count of protein-ligand interactions for the simulation. The upper panel provides an overview of the total count of specific interactions between the protein and the ligand. On the other hand, the lower panel illustrates the residues interacting with the ligand in each trajectory frame. Residues forming multiple specific contacts with the ligand are depicted with a darker shade of orange, as indicated by the scale on the right side of the figure (11).

3.3.8. Protein-Ligand Contacts

During the simulation, monitoring and analyzing interactions between the protein and the ligand are possible. These interactions are classified by type

and depicted in the plot. Protein-ligand interactions, also known as 'contacts,' are categorized into four types: Hydrogen Bonds, Hydrophobic interactions, Ionic interactions, and Water Bridges. The plot indicates that the majority of interactions with amino acid residues involve hydrophobic interactions and water bridging during the simulation period, as shown in Figure 12.

3.3.9. Ligand Torsion Profile

The ligand torsions plot provides an overview of the conformational changes in each rotatable bond (RB) of the ligand throughout the simulation trajectory (from 0.00 to 50.05 nanoseconds). In the top panel, a 2D representation of the ligand illustrates the color-coded rotatable bonds for clarity. Each rotatable bond's torsion is depicted by a dial plot alongside matching colored bar plot. The dial plots visualize the torsion's conformational changes over time, with the simulation's onset at the center and its progression depicted radially outward. Bar plots summarize the data from the dial plots, indicating the probability density of the torsion. If torsional potential data is available, the plot also displays the potential of the rotatable bond by aggregating related torsions' potentials, shown on the left Y-axis in kcal/mol. Analyzing the

histogram and torsion potential relationships provides insights into the conformational strain experienced by the ligand as it maintains its bound conformation to the protein. as shown in Figure 13.

4. Conclusions

The computational analysis presents promising possibilities for the creation of novel lung cancer treatments by targeting the EGFR pathway. Advanced methods such as molecular docking, ADME analysis, and molecular dynamics simulations were used to evaluate eight potential compounds. Docking results showed strong binding of these compounds to EGFR, surpassing erlotinib, indicating their potential effectiveness in targeting a crucial element in lung cancer treatment. ADME analysis revealed favorable pharmacokinetic properties and minimal blood-brain barrier penetration. Molecular dynamics simulations demonstrated a stable ligand-protein complex with minimal fluctuations.

Each compound possesses unique properties that could influence its suitability for drug development, and further experimental assessment focusing on safety, efficacy, and pharmacokinetics is crucial. These findings provide a promising avenue for developing effective lung cancer treatments; however, in vivo studies are essential to confirm the compounds' efficacy and safety. Future research should explore strategies to enhance the design of EGFR inhibitors, aiming for improved potency and selectivity.

ACKNOWLEDGEMENT

The author would like to thank Mustansiriyah University (www.uomustansiriyah.edu.iq) in Baghdad, Iraq, for their support in completing this work.

References

- [1] Bade BC, Cruz CSD. Lung cancer 2020: epidemiology, etiology, and prevention. *Clinics in Chest Medicine* 41 (2020) 1-24.
- [2] Cruz CSD, Tanoue LT, Matthey RA. Lung cancer: epidemiology, etiology, and prevention. *Clinics in Chest Medicine* 32 (2011) 605-644.
- [3] Hasan HA, Ali KF, Mehdi WA. Synthesis, characterization, docking study and biological activities of new 3-aminorhodanine derivatives. *Al Mustansiriyah Journal of Pharmaceutical Sciences* 24 (2024) 299-310.
- [4] Wieduwilt MJ, Moasser MM. The epidermal growth factor receptor family: biology driving targeted therapeutics. *Cellular and Molecular Life Sciences* 65 (2008) 1566-1584.
- [5] Khozin S, Blumenthal GM, Jiang X, He K, Boyd K, Murgo A, et al. U.S. Food and Drug Administration approval summary: Erlotinib for the first-line treatment of metastatic non-small cell lung cancer with epidermal growth factor receptor exon 19 deletions or exon 21 (L858R) substitution mutations. *The Oncologist* 19 (2014) 774-779.
- [6] Madhusudan S, Ganesan TS. Tyrosine kinase inhibitors in cancer therapy. *Clinical Biochemistry* 37 (2004) 618-635.
- [7] Stein RA, Staros JV. Insights into the evolution of the ErbB receptor family and their ligands from sequence analysis. *BMC Evolutionary Biology* 6 (2006) 79.
- [8] Agarwal SM, Nandekar P, Saini R. Computational identification of natural product inhibitors against EGFR double mutant (T790M/L858R) by integrating ADME, machine learning, molecular docking and a dynamics approach. *RSC Advances* 12 (2022) 16779-16789.
- [9] Ismail R, Ismail N, Abuserii S, Abou El Ella DA. Recent advances in 4-aminoquinazoline based scaffold derivatives targeting EGFR kinases as anticancer agents. *Future Journal of Pharmaceutical Sciences* 2 (2016).
- [10] Seshacharyulu P, Ponnusamy MP, Haridas D, Jain M, Ganti AK, Batra SK. Targeting the EGFR signaling pathway in cancer therapy. *Expert Opinion on Therapeutic Targets* 16 (2012) 15-31.
- [11] Jedhe GS, Paul D, Gonnade RG, Santra MK, Hamel E, Nguyen TL, Sanjayan GJ. Correlation of hydrogen-bonding propensity and anticancer profile of tetrazole-tethered combretastatin analogues. *Bioorganic*

- & Medicinal Chemistry Letters 23 (2013) 4680-4684.
- [12] Yadav IS, Singh H, Khan MI, Chaudhury A, Raghava GP, Agarwal SM. EGFRIndb: epidermal growth factor receptor inhibitor database. *Anti-Cancer Agents in Medicinal Chemistry* 14 (2014) 928-935.
- [13] Ahmed M, Sadek MM, Abouzeid KA, Wang F. In silico design: extended molecular dynamic simulations of a new series of dually acting inhibitors against EGFR and HER2. *Journal of Molecular Graphics and Modelling* 44 (2013) 220-231.
- [14] Alonso H, Bliznyuk AA, Gready JE. Combining docking and molecular dynamic simulations in drug design. *Medicinal Research Reviews* 26 (2006) 531-568.
- [15] Zappavigna S, Cossu AM, Grimaldi A, Bocchetti M, Ferraro GA, Nicoletti GF, Filosa R, Caraglia M. Anti-inflammatory drugs as anticancer agents. *International Journal of Molecular Sciences* 21 (2020) 2605.
- [16] Roy HK, Karoski WJ, Ratashak A, Smyrk TC. Chemoprevention of intestinal tumorigenesis by nabumetone: induction of apoptosis and Bcl-2 downregulation. *British Journal of Cancer* 84 (2001) 1412-1416.
- [17] Kumar A, Singh AK, Singh H, Vijayan V, Kumar D, Naik J, et al. Nitrogen containing heterocycles as anticancer agents: a medicinal chemistry perspective. *Pharmaceuticals* 16 (2023) 299.
- [18] Kerru N, Gummidi L, Maddila S, Gangu KK, Jonnalagadda SB. A review on recent advances in nitrogen-containing molecules and their biological applications. *Molecules* 25 (2020) 1909.
- [19] Janowska S, Paneth A, Wujec M. Cytotoxic properties of 1,3,4-thiadiazole derivatives—A review. *Molecules* 25 (2020) 4309.
- [20] Glomb T, Szymankiewicz K, Świątek P. Anti-cancer activity of derivatives of 1,3,4-oxadiazole. *Molecules* 23 (2018) 3361.
- [21] Fu Y, Zhao J, Chen Z. Insights into the molecular mechanisms of protein-ligand interactions by molecular docking and molecular dynamics simulation: a case of oligopeptide binding protein. *Computational and Mathematical Methods in Medicine* 2018 (2018) 3502514
- [22] Patil R, Das S, Stanley A, Yadav L, Sudhakar A, Varma AK. Optimized hydrophobic interactions and hydrogen bonding at the target-ligand interface leads the pathways of drug-designing. *PLOS ONE* 5 (2010) e12029.
- [23] Chen X, Li H, Tian L, Li Q, Luo J, Zhang Y. Analysis of the physicochemical properties of acaricides based on Lipinski's rule of five. *Journal of Computational Biology* 27 (2020) 1397-1406.